JCI The Journal of Clinical Investigation

Mechanisms of insulin resistance in experimental hyperinsulinemic dogs.

P D Miles, … , A R Moossa, J M Olefsky

J Clin Invest. 1998;101(1):202-211. https://doi.org/10.1172/JCI1256.

Research Article

This study was undertaken to characterize the insulin resistance and the mechanism thereof caused by chronic hyperinsulinemia produced in dogs by surgically diverting the veins of the pancreas from the portal vein to the vena cava. Pancreatic venous diversion (PVD, n = 8) caused a sustained increase in arterial insulin and decrease in portal insulin concentration compared with the control group (n = 6). Hyperinsulinemic euglycemic clamps were conducted 4 wk after surgery. The increase in the glucose disposal rate (GDR) was significantly less in the PVD group (39.0+/-5.0 vs. 27.9+/-3.2 micromol/kg/min, P < 0.01) compared with the control group, but the suppression of hepatic glucose production by insulin was similar for both groups. Muscle insulin receptor tyrosine kinase activity (IR-TKA) increased from 6.2+/-0.4 to 20.3+/-2.7 in the control group, but from 5.8+/-0.5 to only 12.7+/-1.7 fmol P/fmol IR in the PVD group (P < 0.01). With respect to the periphery, the time to half-maximum response (t1/2a) for arterial insulin was the same for both groups, whereas the t1/2a for lymph insulin (30+/-3 vs. 40+/-4 min, P < 0.05) and GDR (29+/-3 vs. 66+/-10 min, P < 0.01) were greater for the PVD group. Chronic hyperinsulinemia led to marked peripheral insulin resistance characterized by decreased insulin-stimulated GDR, and impaired activation of GDR kinetics due, in part, to reduced IR-TKA. Transendothelial […]

Mechanisms of Insulin Resistance in Experimental Hyperinsulinemic Dogs

Philip D.G. Miles,* Shujun Li,* Marquis Hart,* Oreste Romeo,* Jean Cheng,* Aaron Cohen,* Karim Raafat,* A.R. Moossa,* and Jerrold M. Olefsky[‡§‖]

**Department of Surgery and ‡Department of Medicine, University of California, San Diego; §San Diego Veterans Affairs Medical Center; and ‖Whittier Diabetes Institute, Division of Endocrinology and Metabolism, La Jolla, California 92093*

Abstract

This study was undertaken to characterize the insulin resistance and the mechanism thereof caused by chronic hyperinsulinemia produced in dogs by surgically diverting the veins of the pancreas from the portal vein to the vena cava. Pancreatic venous diversion (PVD, $n = 8$) caused a sustained increase in arterial insulin and decrease in portal insulin concentration compared with the control group ($n = 6$). Hyperinsulinemic euglycemic clamps were conducted 4 wk after surgery. The increase in the glucose disposal rate (GDR) was significantly less in the PVD group (39.0±5.0 vs. 27.9±3.2 μmol/kg/min, $P < 0.01$) compared with the control group, but the suppression of hepatic glucose production by insulin was similar for both groups. Muscle insulin receptor tyrosine kinase activity (IR-TKA) increased from 6.2±0.4 to 20.3±2.7 in the control group, but from 5.8±0.5 to only 12.7±1.7 fmol P/fmol IR in the PVD group ($P < 0.01$). With respect to the periphery, the time to half-maximum response ($t_{1/2}$a) for arterial insulin was the same for both groups, whereas the $t_{1/2}$a for lymph insulin (30±3 vs. 40±4 min, $P < 0.05$) and GDR (29±3 vs. 66±10 min, $P < 0.01$) were greater for the PVD group. Chronic hyperinsulinemia led to marked peripheral insulin resistance characterized by decreased insulin-stimulated GDR, and impaired activation of GDR kinetics due, in part, to reduced IR-TKA. Transendothelial insulin transport was impeded and was responsible for one third of the kinetic defect in insulin-resistant animals, while slower intracellular mechanisms of GDR were responsible for the remaining two thirds. (*J. Clin. Invest.* 1998. 101:202–211.) Key words: insulin resistance • hyperinsulinemia • transendothelial insulin transport • insulin kinetics • glucose clamp

Introduction

The lack of a large animal model of insulin resistance has undoubtedly hindered the scientific investigation into disorders of insulin action such as non–insulin-dependent diabetes mellitus (NIDDM)[1] and obesity. However, the treatment of insulin-dependent diabetes mellitus (IDDM) by pancreas transplantation raises an interesting possibility. The procedure usually entails connecting the venous drainage of the donor pancreas to the systemic circulation of the recipient instead of the anatomically correct portal vein because of surgical limitations (1). The liver normally extracts ~ 50% of the insulin on its first pass; therefore, bypass of the liver leads to systemic hyperinsulinemia, which is known to be sufficient to cause insulin resistance (2, 3).

To minimize the confounding effects of pancreas transplantation (e.g., denervation of pancreas and immunosuppression), Radziuk and colleagues (4) performed in situ pancreas transplants in the dog whereby the pancreas stayed in place and only the venous drainage of the pancreas was surgically diverted from the portal vein to the inferior vena cava. These animals were hyperinsulinemic and, indeed, insulin resistant but remained glucose tolerant. Both insulin resistance and hyperinsulinemia frequently precede the development of NIDDM. Epidemiological studies (for reviews, see references 5 and 6) indicate that insulin resistance may be the primary defect of NIDDM, since it can be detected in most prediabetic patients long before the deterioration of glucose tolerance, often occurring when insulin secretion is actually increased. The hyperinsulinemic dog resembles certain early features of the prediabetic and, therefore, may serve as a large animal model of NIDDM. This study was undertaken to characterize the insulin resistance caused by pancreatic venous diversion (PVD) in the dog and to determine the mechanism of the resistance.

Another important aspect of insulin resistance is decreased kinetics of insulin action. Not only are the glucose metabolic responses to insulin reduced in NIDDM and obesity, it takes longer for insulin to act (7, 8). Under normal physiological conditions, the increase in glucose disposal rate (GDR) naturally lags behind the increase in circulating insulin levels, and it has been shown to occur before insulin receptor binding (9–11). Previously, we have confirmed that this rate-limiting step in insulin's peripheral action is transendothelial insulin transport: the movement of plasma across the capillary endothelium and into the interstitial fluid compartment of skeletal muscle (12). Therefore, the kinetics of insulin action and transendothelial insulin transport were also examined during the development of insulin resistance caused by chronic hyperinsulinemia in this study.

Sustained elevation of circulating insulin was achieved by transposing the veins of the pancreas from the portal vein to the vena cava (13), thus avoiding first-pass extraction of insulin by the liver. The kinetics of insulin and its biological effects

Address correspondence to Philip D.G. Miles, Ph.D., Department of Surgery (8400), UCSD Medical Center, 200 West Arbor Dr., San Diego, CA 92103.

Received for publication 21 July 1997 and accepted in revised form 28 October 1997.

The Journal of Clinical Investigation
Volume 101, Number 1, January 1998, 202–211
http://www.jci.org

1. *Abbreviations used in this paper:* GDR, glucose disposal rate; HGP, hepatic glucose production; IR-TKA, insulin receptor tyrosine kinase activity; IVGTT, intravenous glucose tolerance test; NIDDM, non–insulin-dependent diabetes mellitus; $t_{1/2}$a, time to maximum response; TLI, trypsin-like immunoreactivity.

were measured during hyperinsulinemic (~ 600 pmol/liter) euglycemic glucose clamp experiments. The time course of insulin action in muscle was assessed by comparing the temporal relationship between changes in arterial and lymph insulin concentrations, and whole body GDR, whereby the dynamics of lymph insulin are indicative of insulin receptor binding (12). With respect to the liver, the time course of insulin action was assessed by comparing the temporal relationship between changes in portal insulin concentration, and hepatic glucose production (HGP).

Methods

Overview. Studies were conducted on chronically prepared, male mongrel dogs (n = 14) weighing 20.8–28.0 kg. Animals were housed under controlled temperature and light (12 h light, 12 h dark) conditions with water ad libitum, and were fed once per day a diet of dry chow (Iams Chunks, 26% protein, 15% fat, 5% fiber, 10% moisture; The Iams Company, Dayton, OH). Animals were fasted for 18 h before surgery, and a blood sample for glucose and insulin determination was taken percutaneously. Under general anesthesia, surgery was performed to divert the venous drainage of the pancreas (PVD group, n = 8) or to leave it intact in a sham operation (control group, n = 6) (see below). Prophylactic antibiotics included clindamycin (300 mg intravenous [i.v.]), gentamicin (80 mg i.v.), and benzathine penicillin (1.2×10^6 U intramuscular [i.m.]). On the first postoperative day, the dogs were treated with heparin (1,000 U/d, subcutaneous [s.c.]) for 4 d and with acetylsalicylic acid (325 mg/d by mouth) each day thereafter. Normal food intake was resumed by the second postoperative day. The animals were monitored closely for 4 wk after the surgery, and fasted blood samples were collected on days 0 (preoperative), 3, 7, 14, and 28 for the determination of plasma glucose and insulin. Additional blood samples were drawn on days 0 and 7 for the determination of trypsin-like immunoreactivity (TLI; exocrine pancreatic test) and serum cobalamin and folate (intestinal function test). On day 28, all dogs underwent an intravenous glucose tolerance test (IVGTT) to assess β cell function (see below). 3–4 d later, whole body insulin sensitivity was measured using the hyperinsulinemic euglycemic glucose clamp technique (see below). All procedures were in accordance with the Guide for the Care and Use of Laboratory Animals of the National Institutes of Health and approved by the Animal Subjects Committee of the University of California, San Diego.

PVD operation. Surgery was performed to transpose the pancreatic gastroduodenal vein and the gastrosplenic vein from the portal vein to the inferior vena cava as described previously (4). Briefly, general anesthesia was induced with thiopental sodium (20 mg/kg i.v.; Abbot Laboratories, North Chicago, IL) followed by intubation, mechanical ventilation, and inhalation of halothane (1–1.5% in room air). The pancreas was exposed through a midline abdominal incision. The pancreatic branches of the inferior pancreaticoduodenal vein were ligated at their entrance into the pancreas. The head of the pancreas was dissected from the duodenum, ligating small venous branches except for a small area surrounding the major pancreatic duct. The arterial circulation and its accompanying neural input to the pancreas were left intact. The portal vein was then isolated from the porta hepatis, and the common bile duct was left intact. The gastroduodenal and gastrosplenic veins were isolated from their entrance into the portal vein, and the inferior vena cava was mobilized for ~ 4 cm above the renal veins. The portal vein was partially occluded at the origins of the gastroduodenal and gastrosplenic veins, and heparin (1,500 U) was given i.v. The veins were clamped, transected, and anastomosed to the inferior vena cava in an end-to-side fashion.

Pancreatic sham (control) operation. The animals of this group were prepared exactly as described above, except that the gastroduodenal and gastrosplenic veins of the pancreas were left attached to the portal vein.

IVGTT. Animals underwent an IVGTT to assess endogenous pancreas function. Briefly, a percutaneous i.v. line (16-gauge angiocatheter) was placed in the cephalic vein of the conscious dog and used for both injection and blood sampling. Two basal blood samples were drawn. A standard glucose challenge (0.3 g/kg; 50% dextrose) was given i.v. at time 0. Blood samples were then drawn frequently over a period of 60 min for the measurement of plasma glucose, insulin, and C-peptide.

Hyperinsulinemic euglycemic glucose clamp and surgical preparation. Surgery was performed under general anesthesia to implant three infusion and three sampling catheters. After an overnight fast, anesthesia was induced with 30 mg/kg pentobarbital sodium (Nembutal; Abbot Laboratories) administered i.v. The dog was intubated and ventilated with room air. Anesthesia was maintained with 2 mg/kg/h pentobarbital, while normal saline containing 1,000 U/liter heparin was given i.v. to maintain body fluid volume (~ 300 ml/h) and patency of the thoracic duct catheter.

The right jugular vein was mobilized through a neck incision. Three polyvinylchloride catheters (Tygon® Micro-bore; 0.03″ ID, 0.09″ OD; Norton, Akron, OH) were inserted into the vessel, advanced into the superior vena cava, and secured in place. These catheters were used for the infusion of tracer, insulin, and glucose. A longitudinal incision was made on the left side of the neck parallel to the internal jugular vein to expose the thoracic duct beneath the junction of the internal jugular and subclavian veins. The duct was cannulated with polyethylene tubing (Intramedic PE-60; Clay Adams, Parsippany, NJ), and the lymph was allowed to drain freely for the continuous sampling of lymph insulin. Through the same incision, the left carotid artery was mobilized and cannulated (Pharmaseal extension tube; Baxter Healthcare Corp., Valencia, CA). The tip of the catheter was advanced into the aortic arch and secured in place. This catheter was used for sampling of arterial blood. A midline abdominal incision was made to access the portal vein blood. A large mesenteric vein was mobilized and cannulated with a Tygon® catheter (0.05″ ID, 0.09″ OD; Norton). The tip of the catheter was advanced proximally into the portal vein to the base of the liver and secured in place. Bilateral incisions were made on the ventral aspect of the upper hind limbs to gain access to the quadriceps muscle. Discrete muscle groups were dissected apart and cleared of connective tissue to ensure uncontaminated muscle biopsies. All neck incisions were sutured closed, while the abdominal and leg incisions were packed with saline soak gauze to reduce evaporation.

After catheter placement, a 6-h experiment commenced which consisted of a 120-min equilibration period, followed by a 30-min basal period and a 160-min activation phase (infusion of insulin). The experiment was begun at time −120 min with a priming injection (25 μCi/5 ml) and a constant infusion (0.25 μCi/min) of D-[3-^{3}H]glucose (New England Nuclear, Boston, MA). Tracer was diluted to 5 μCi/ml in a solution containing 100 mg/dl unlabeled D-glucose (Mallinckrodt Inc., Paris, KY) as carrier and 200 mg/dl sodium benzoate (Mallinckrodt Inc.) as a preservative. After the 2-h tracer-equilibration period, arterial blood samples (3 ml) were taken at −30, −20, −10, and 0 min for the immediate determination of plasma glucose concentration and subsequent determination of glucose specific activity. Beginning at time 0 and continuing for 160 min, insulin was infused at 7.2 nmol/kg/min. The insulin infusate was prepared from regular human insulin (Novolin R, 100 U/ml; Novo Nordisk Pharmaceuticals Inc., Princeton, NJ) in 50 ml of normal saline containing 2 ml of the dog's own plasma. Arterial blood samples (3 ml) were taken at 2.5, 5, 10, 15, and 20 min, and every 10 min between 20 and 160 min. A portion (200 μl) of these samples was used for the immediate determination of blood glucose. Based on these values, plasma glucose was clamped at basal by a variable glucose infusion (50% dextrose; Abbot Laboratories). As recommended previously (14), a quantity of tracer was added to the glucose infusate to avoid rapid dilution of the labeled glucose pool with unlabeled glucose. In addition to these blood samples, extra arterial blood (3 ml), portal blood (3 ml), and thoracic duct lymph (1.5 ml) samples were taken for the determination of insulin concen-

tration at −30, −10, 5, 10, 20, 30, 40, 60, 80, 100, 130, and 160 min. Muscle biopsies (1 g) were taken for the determination of insulin receptor tyrosine kinase activity (IR-TKA) at time −30, −10, 130, and 160 min.

Blood samples collected for the determination of specific activity were placed in gray top Vacutainers (Becton Dickinson, Inc., Rutherford, NJ), while those collected for the determination of insulin concentration were placed in red top Vacutainers and allowed to clot. Sampling of lymph was accomplished by letting it drip into microcentrifuge tubes beginning 30 s earlier and ending 30 s later than the sampling time. The flow rate was generally > 1 ml/min. All blood and lymph samples were refrigerated until centrifugation, and upon subsequent separation were stored at −70°C for latter assays. Muscle biopsies were taken alternatively from each of the quadriceps muscles, making sure these serial tissue samples were sufficiently separated. Once taken, the biopsies were dropped immediately into liquid nitrogen and subsequently stored at −70°C to preserve insulin receptor kinase activity. The animal was killed immediately at the end of the experiment.

Assays

Plasma glucose was assayed by the glucose oxidase technique on an automated analyzer (model 23A; Yellow Springs Instrument Co., Yellow Springs, OH). Insulin concentrations in serum and lymph were measured in duplicate using a double antibody RIA (15). For the determination of [3-^{3}H]glucose in plasma, samples were measured in duplicate after deproteination with perchloric acid (16). C-peptide values were determined in the laboratory of K. Polonsky (17, 18). Insulin receptor kinase activities of muscle were assayed as outlined previously (10). In vivo IR-TKA was preserved in vitro by freezing the tissue sample immediately in liquid nitrogen and then subsequently thawing the sample in the presence of phosphatase inhibitors for in vitro IR-TKA measurement. Activity is expressed as the ability of the receptor (20 fmol) to phosphorylate an exogenous substrate, histone 2B.

Data analysis. Plasma glucose and tracer data were analyzed after smoothing by the OOPSEG computer program (19). GDR and HGP were calculated according to Steele's equation (20) as modified for labeled glucose infusion (21).

Values presented are mean±SEM. Rates of activation ($t_{1/2}$a) were calculated by estimating the time to reach half-maximum response after the start of insulin infusion for each individual experiment. Statistical tests were performed using two-way ANOVA for balanced and unbalanced data. Significance was assumed at $P < 0.05$.

Results

Exocrine pancreas and intestinal function

Canine TLI measurements for both experimental groups were in the normal range, indicating normal exocrine pancreatic function. The TLI level of the PVD group was similar to that of the control group before (21.2±1.3 vs. 17.8±2.0 μg/liter, NS) and 1 wk after surgery (19.1±2.8 vs. 16.6±2.2 μg/liter, NS). Also, intestinal function of both groups appeared normal, as indicated by plasma cobalamin and folate levels. There was no significant difference in these plasma substrates before or after surgery or between the two groups.

Postsurgical follow-up

As seen in Fig. 1, the postoperative plasma insulin and glucose concentrations of the control group remained at presurgery levels. Conversely, diversion of the venous drainage of the pancreas led to systemic hyperinsulinemia while glucose remained essentially unchanged. Insulin levels of the PVD group rose from 41±5 to 97±24 pmol/liter ($P < 0.05$) by postsurgical day 3, and declined slowly and steadily thereafter (Fig. 1 *B*).

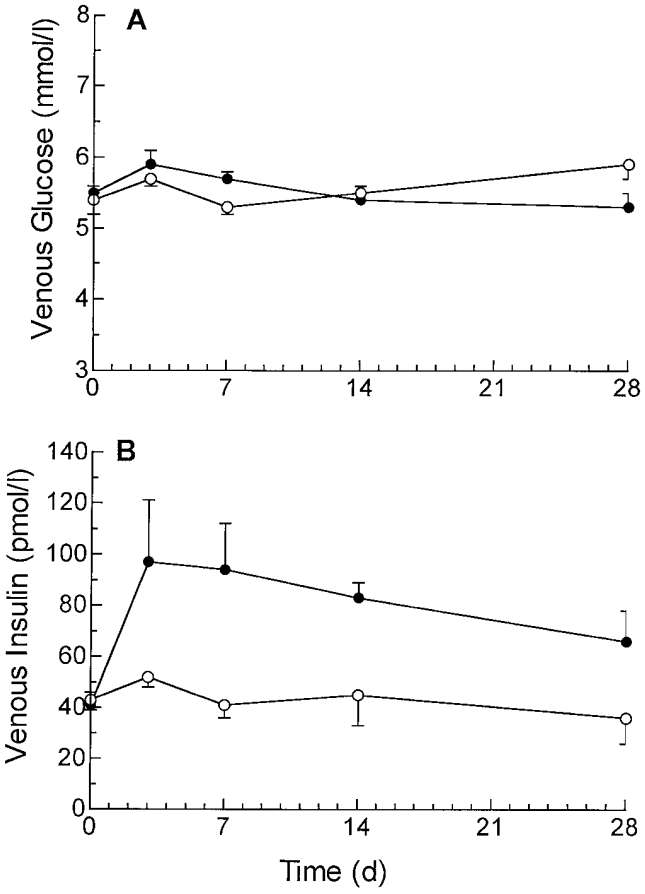

Figure 1. (*A*) Plasma venous glucose and (*B*) insulin concentrations measured over a 4-wk period in sham-operated (○) and PVD animals (●).

IVGTT

Endocrine function of the pancreas was tested with the IVGTT as seen in Fig. 2. As expected, the i.v. injection of glucose resulted in a marked increase and gradual decline to basal levels in the plasma venous glucose, insulin, and C-peptide concentrations of the PVD and control groups. The circulating glucose excursion levels of the two groups (Fig. 2 *A*) were essentially identical, demonstrating that the PVD group was glucose tolerant. However, this tolerance was at the expense of much higher insulin levels. In response to the glucose challenge, the rise in venous insulin (Fig. 2 *B*) of the PVD group (72±18 to 447±53 pmol/liter) was greater than that of the control group (38±11 to 307±35 pmol/liter, $P < 0.01$). Conversely, the rise in C-peptide levels (Fig. 2 *C*) of the PVD group (0.130±0.018 to 0.508±0.055 pmol/ml) was on average slightly less than the control group (0.164±0.016 to 0.565±0.061 pmol/ml, $P < 0.05$), which indicates that β cell insulin secretion was not increased in the PVD animals and that the hyperinsulinemia was due to decreased insulin clearance as a result of the liver bypass.

Hyperinsulinemic euglycemic glucose clamps

Basal values. The basal glucose concentrations of the PVD (6.3±0.1 mmol/liter) and control groups (6.4±0.2 mmol/liter, NS) were similar, and both were maintained near 5.6 mmol/liter throughout the glucose clamp (Table I). As seen in Table I

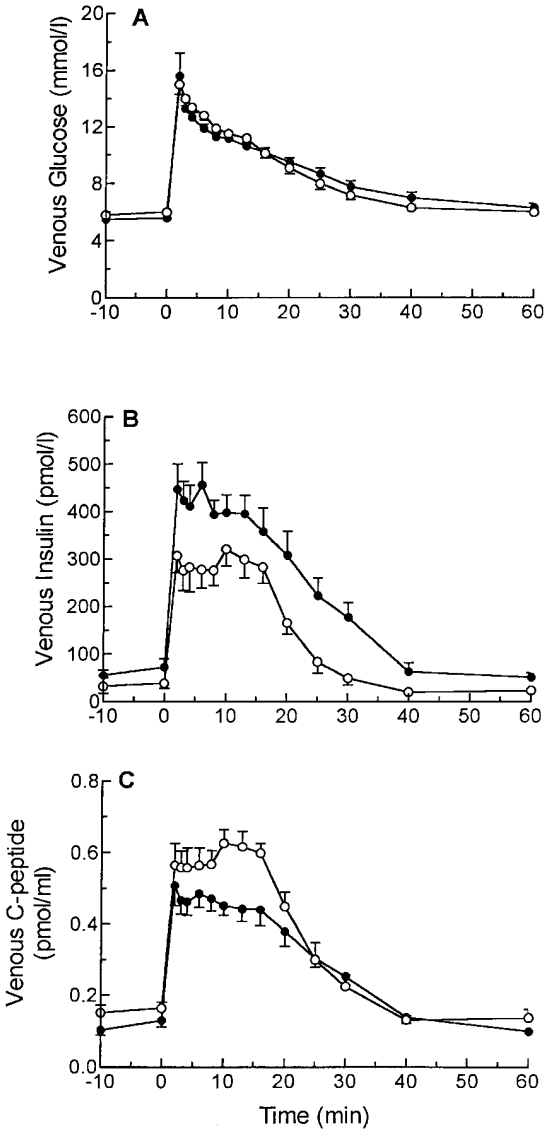

Figure 2. (*A*) Plasma venous glucose, (*B*) insulin, and (*C*) C-peptide concentrations taken during an IVGTT. Dextose (0.3 g/kg) was given at time 0. ○, Control group. ●, PVD group.

and Fig. 3 *A*, the normal basal portal-arterial-lymph insulin gradient is clearly visible in the control group. Basal portal insulin (201±45 pmol/liter) was markedly greater than arterial insulin (51±9 pmol/liter, $P < 0.01$), which in turn was significantly greater than lymph insulin concentration (30±12 pmol/liter, $P < 0.05$). As expected, the portal-peripheral gradient was reversed in the PVD group. Venous diversion of the pancreas into the systemic circulation resulted in systemic hyperinsulinemia and hepatic hypoinsulinemia. Arterial insulin (99±24 vs. 51±9 pmol/liter, $P < 0.05$) and lymph insulin concentrations (60±12 vs. 30±12 pmol/liter, $P < 0.05$) of the PVD group were significantly greater than in the control group (Table I and Fig. 3 *B*). Conversely, portal insulin levels of the PVD group (54±6 vs. 201±45 pmol/liter, $P < 0.01$) were markedly less than the control group (Table I). Despite the altered insulin gradient, there was no significant difference between the two groups in basal glucose turnover, as seen in Table I (GDR, 14.2±0.8 vs. 14.0±1.4 μmol/kg/min, NS; HGP, 13.5±0.6 vs. 13.6±1.4 μmol/kg/min, NS).

Table I. Basal and Hyperinsulinemic Euglycemic Glucose Clamp Steady State Values (Mean±SEM) of PVD Group (n = 8) and Control Group (n = 6)

	Basal		Insulin infusion	
	Control	PVD	Control	PVD
Glucose (mmol/liter)	6.4±0.2	6.3±0.1	5.6±0.1	5.6±0.1
Insulin (pmol/liter)				
Arterial	51±9	99±24*	489±42	540±45
Portal	201±45	54±6*	378±48	402±30
Lymph	30±12	60±12*	246±24	240±24
Glucose turnover (μmol/kg/min)				
GDR	14.0±1.4	14.2±0.8	39.0±5.0	27.9±3.2*
HGP	13.6±1.4	13.5±0.6	3.4±1.4	3.9±1.0
IR-TKA (fmol P/fmol IR)	6.2±0.4	5.8±0.5	20.3±2.7	12.7±1.7*

The glucose clamp consisted of an activation phase, during which insulin was infused at 7.2 nmol/kg/min. *Significantly different from control group ($P < 0.05$).

Response to insulin infusion. After the start of the peripheral insulin infusion, arterial and portal insulin concentrations of both groups rose rapidly to steady state levels, and were near maximal 5 min into the infusion (Fig. 3, *A* and *B*). The portal levels remained significantly lower than the arterial levels throughout the activation period ($P < 0.01$). In contrast, the concentration of lymph insulin in both groups rose much more slowly, and reached a plateau only half that of the arterial concentration ($P < 0.001$). In the PVD group, the steady state arterial (540±45 vs. 489±42 pmol/liter, NS), portal (402±30 vs. 378±48 pmol/liter, NS), and lymph insulin concentrations (240±24 vs. 246±24 pmol/liter, NS) matched the respective values of the control group, as seen in Table I.

Changes in glucose turnover in response to a physiological infusion of insulin can be seen in Fig. 3, *C* and *D*. GDR of the control group increased to reach a steady state level of 39.0±5.0 μmol/kg/min, whereas it only reached a level of 27.9±3.2 μmol/kg/min in the PVD group ($P < 0.01$). HGP declined to a similar level in both the control (3.4±1.4 μmol/kg/min) and PVD groups (3.9±1.0 μmol/kg/min, NS).

IR-TKA. We have developed previously a method to measure the ability of insulin to stimulate in vivo the in situ tyrosine kinase activity of skeletal muscle insulin receptors. With this approach, muscle samples are obtained at the end of the glucose clamp period, and insulin receptors are isolated under conditions that preserve the kinase activation state that existed at the time of in vivo tissue sampling (10). This provides a measurement of the effect of the insulin infusion, given during the glucose clamp to activate skeletal muscle insulin receptor kinase activity. As seen in Fig. 4, with this approach, muscle IR-TKA increased from 6.2±0.4 to 20.3±2.7 fmol P/fmol IR in the control group, but increased from 5.8±0.5 to only 12.7±1.7 fmol P/fmol IR in the PVD group ($P < 0.01$). Since there was no significant difference in the total number of insulin receptors between the PVD (705±124) and control groups (767±116 fmol IR/g muscle), these results indicate that the chronic hyperinsulinemia induced by PVD causes impaired IR-TKA, which provides at least one mechanism for the PVD-induced insulin-resistant state.

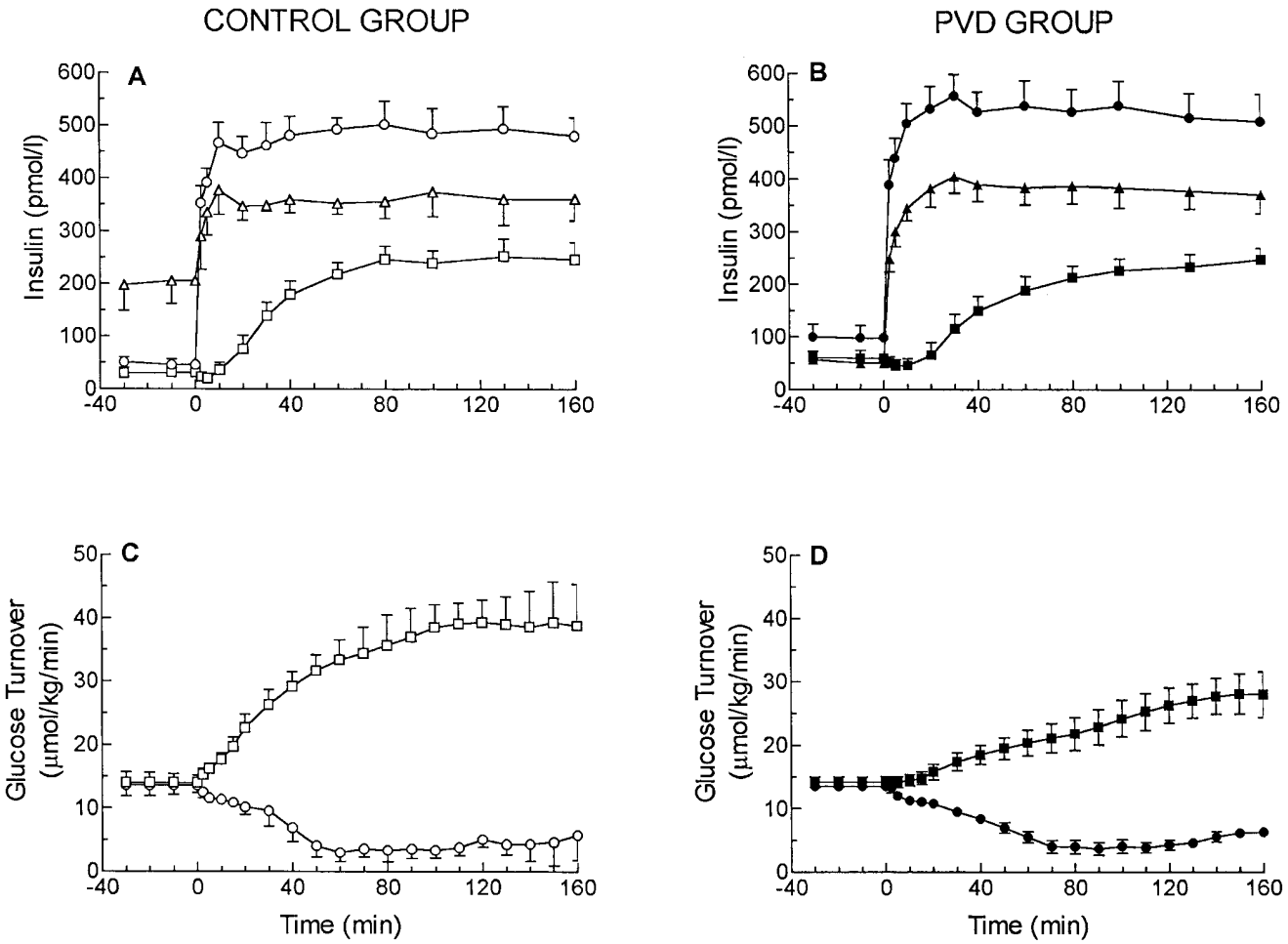

Figure 3. (*A*) Arterial (○), portal (△), and lymph (thoracic duct, □) insulin concentrations and (*C*) GDR (□) and HGP (○) of the control animals during 100 min i.v. infusion of insulin (7.2 nmol/kg/min). Mean±SEM (n = 8). (*B*) Arterial (●), portal (▲), and lymph (thoracic duct, ■) insulin concentrations and (*D*) GDR (■) and HGP (●) of the PVD animals during 100 min i.v. infusion of insulin (7.2 nmol/kg/min). Mean±SEM (n = 6).

Temporal comparison of PVD and control groups. To compare directly the kinetics of the respective response curves of the two groups, the data were expressed as percentage of maximum response (Fig. 5). The rate of increase of arterial insulin (Fig. 5 *A*) and portal insulin (Fig. 5 *B*) of the PVD group was essentially identical to that of the control group. However, as seen in Fig. 5 *C*, the lymph insulin response curve of the PVD group was markedly slower than that of the control group (see below for statistical comparison).

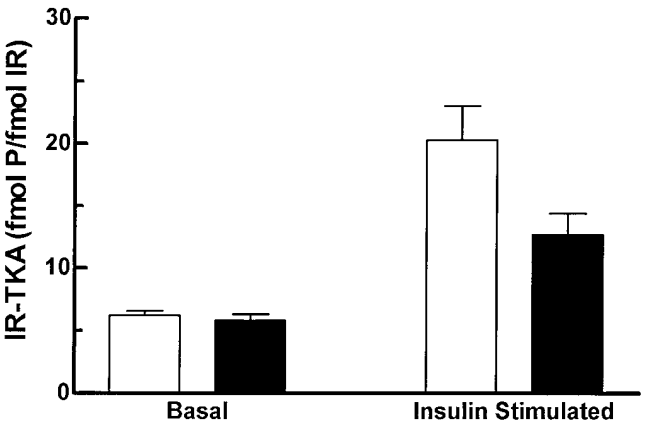

Figure 4. Muscle IR-TKA of control (*white bars*, n = 8) and PVD (*black bars*, n = 6) animals during 100 min i.v. infusion of insulin (7.2 nmol/kg/min). Mean±SEM.

The progress curves for stimulation of GDR and suppression of HGP are shown in Fig. 6, *A* and *B*, and are presented as percentage of the maximal stimulation (GDR) or suppression (HGP) achieved. The rate of increase in GDR of the PVD group was markedly slower than that of the control group (Fig. 6 *A*). Conversely, the HGP response curves of both groups were comparable (Fig. 6 *B*).

Rates of activation in response to insulin infusion. To better quantify the relationships depicted in Figs. 5 and 6, the rates of activation were estimated as the average time to reach half-maximum response ($t_{1/2}$a) after the start of insulin infusion. These values are categorized according to whether they pertain to the peripheral circulation (arterial and lymph insulin and GDR) or the hepatic circulation (portal insulin and HGP), and are shown in Table II.

In the control group, the $t_{1/2}$a for GDR (29±3 min) and HGP (33±4 min) were similar (NS). Furthermore, the $t_{1/2}$a for GDR (29±3 min) and lymph insulin (30±3 min, NS) were not

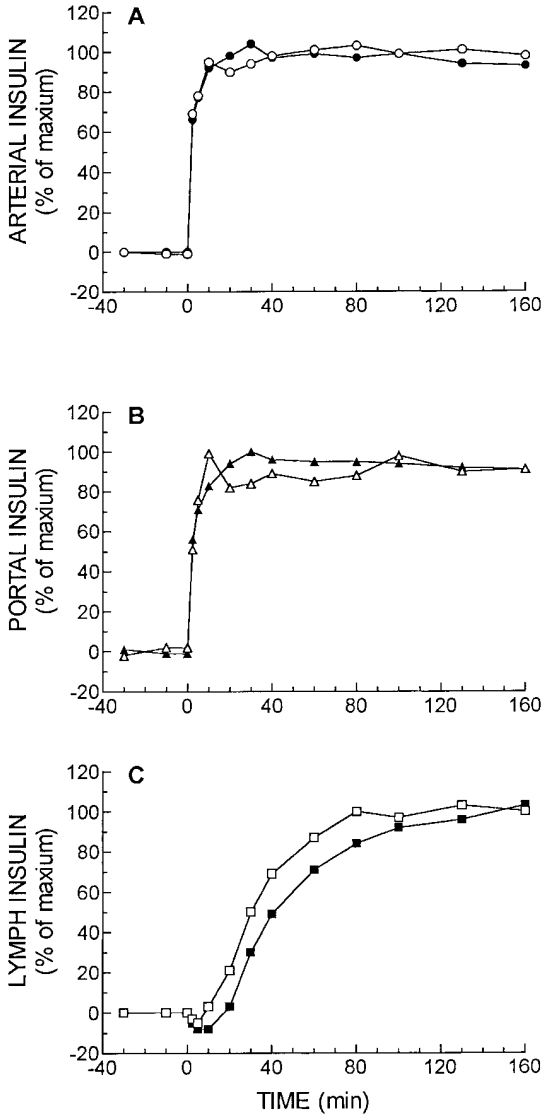

Figure 5. (*A*) Arterial, (*B*) portal, and (*C*) lymph insulin concentrations in response to an i.v. insulin infusion (7.2 nmol/kg/min). All values are represented as a percentage of their maximal response. For clarity, the error bars have been omitted. *Open symbols*, Control group. *Filled symbols*, PVD group.

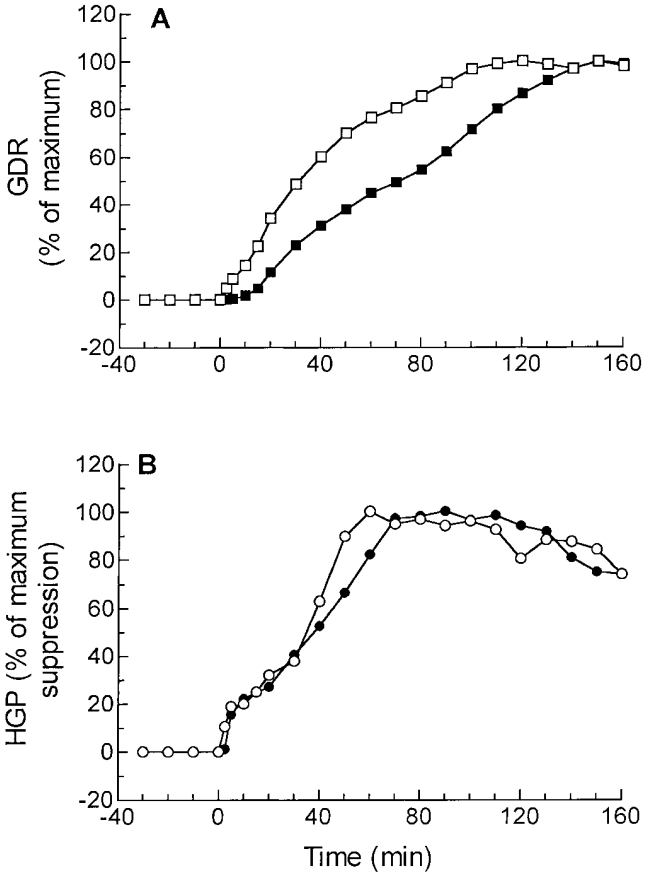

Figure 6. (*A*) GDR and (*B*) HGP responses to an i.v. insulin infusion (7.2 nmol/kg/min). All values are represented as a percentage of their maximal response. The maximum decline in HGP was expressed as 100%. For clarity, the error bars have been omitted. *Open symbols*, Control group. *Filled symbols*, PVD group.

significantly different from one another, and were both markedly greater than that for arterial insulin (2±1 min, $P < 0.01$). The $t_{1/2}$a for portal insulin (2±2 min) was substantially less than for HGP (33±4 min, $P < 0.01$) in the control group. In the PVD group, the $t_{1/2}$a for GDR (66±10 min) was markedly greater than for HGP (35±4 min, $P < 0.01$). Furthermore, the $t_{1/2}$a for GDR (66±10 min) was greater than for lymph insulin (40±4 min, $P < 0.05$), which in turn was greater than for arterial insulin (2±1 min, $P < 0.01$). The $t_{1/2}$a for portal insulin (2±2 min) was substantially less than for HGP (35±4 min, $P < 0.01$).

Thus, with respect to the liver, a direct comparison between groups shows that the respective $t_{1/2}$a values for portal insulin and HGP were similar. The same comparison for the periphery reveals that the $t_{1/2}$a values for arterial insulin (2±1 vs. 2±1 min, NS) are similar, but that the $t_{1/2}$a values for lymph insulin (40±4 vs. 30±3 min, $P < 0.05$) and GDR (66±10 vs. 29±3 min, $P < 0.01$) of the PVD group are both substantially greater than for the control group.

Discussion

In this study, we have generated a large animal model of insulin resistance by creating primary experimental hyperinsulinemia via surgically induced liver bypass of the pancreatic venous

Table II. Time to Reach Half-maximum Response during Insulin Infusion ($t_{1/2}$a)

	Peripheral tissue			Liver	
Group	Arterial insulin	Portal insulin	HGP	Lymph insulin	GDR
Control	2±1	2±2	33±4	30±3	29±3
PVD	2±1	2±2	35±5	40±4*	66±10*‡

The glucose clamp consisted of an activation phase, during which insulin was infused at 7.2 nmol/kg/min. *Significantly different from control ($P < 0.05$). ‡Significantly different from lymph insulin ($P < 0.01$).

drainage in dogs. This produces a canine model of insulin resistance, without the use of pharmacologic agents, and earlier work by Radziuk et al. (4) has shown that portal venous bypass can lead to impaired in vivo insulin action. This canine model is useful in studying the mechanisms of hyperinsulinemia-induced metabolic alterations which may prove relevant to the mechanisms of hyperinsulinemic, insulin-resistant conditions in humans. Our current results show that PVD leads to chronic systemic hyperinsulinemia which produces a marked state of peripheral insulin resistance while hepatic insulin sensitivity remains normal. This peripheral insulin resistance is coincident with a defect in the ability of insulin to stimulate IR-TKA in vivo, and is also associated with striking abnormalities in the kinetics of transendothelial passage of insulin from the vascular space and stimulation of skeletal muscle glucose uptake.

The principles underlying this approach are that the liver extracts at least 50% of secreted insulin on first passage, so that surgical bypass of the liver should result in systemic hyperinsulinemia. Furthermore, chronic hyperinsulinemia has been shown to cause insulin resistance (2, 3). Indeed, hyperinsulinemia and insulin resistance were clearly evident in the PVD animals. The systemic insulin concentration almost doubled after surgery, and this elevated level persisted throughout the 4-wk experimental period. By the fourth postoperative week, peripheral insulin resistance had developed. As seen in the glucose clamp experiments, insulin-stimulated glucose disposal was reduced by $\sim$ 50% in the PVD group. Interestingly, the glucose excursion was normal during the IVGTT, indicating the PVD animals were resistant to insulin but remained glucose tolerant.

As a general view, insulin resistance can be due to prereceptor, receptor, or postreceptor abnormalities, and the current results shed some light on the operative mechanisms in this model. For example, Yang et al. (9), as well as our laboratory (10, 12), have shown previously that the lymph insulin concentration provides a measure of interstitial insulin bathing skeletal muscle, and reflects transendothelial passage of insulin from the circulation to the interstitial space. As seen in Table I and Fig. 3, the lymph insulin concentration of the PVD group was the same as that of the control group during the glucose clamp studies at steady state, indicating that prereceptor abnormalities do not account for the reduced insulin-stimulated steady state GDR values in the PVD dogs.

In contrast, we found good evidence for a decrease in insulin receptor function. During the glucose clamp studies, insulin was infused at a rate of 7.2 nmol/kg/min, and skeletal muscle samples were obtained at the end of the infusion period. In vivo, insulin stimulates IR-TKA, and to measure this, muscle tissue was snap-frozen immediately in liquid nitrogen and subsequently thawed in the presence of protease and phosphatase inhibitors to preserve the in situ insulin receptor activation state which is then assessed by measuring the ability of purified receptors to phosphorylate an artificial substrate (histone 2B) in vitro. These results demonstrated that the insulin infusion stimulated IR-TKA from 6.2±0.4 to 20.3±2.7 fmol P/fmol IR in control animals. In contrast, IR-TKA increased only from 5.8±0.5 to 12.7±1.7 fmol P/fmol IR in the PVD group, demonstrating that this effect of insulin was blunted in the hyperinsulinemic, insulin-resistant animals. It should be noted that this defect is not due simply to a decrease in insulin receptor number, since the kinase data are normalized to insulin receptor content, and, therefore, represent a defect in the intrinsic tyrosine kinase activity of skeletal muscle insulin receptors from PVD dogs. Since we have shown previously a strong correlation between activation of skeletal muscle IR-TKA and insulin-stimulated GDR in both dogs (12) and humans (11), these data indicate that decreased IR-TKA is an important mechanism causing the insulin resistance in these animals. Although impaired IR-TKA appears to be an important mechanism for insulin resistance in this hyperinsulinemic dog model, this does not eliminate the possibility that additional, postreceptor abnormalities exist. Indeed, in vitro studies have demonstrated that chronic incubation of cells with high levels of insulin can lead to multiple defects in insulin action distal to the insulin receptor (22). For example, in these studies, in addition to the deficit in steady state insulin-stimulated glucose disposal rates, there was also a decrease in the rate at which insulin activates GDR. Although it is possible that the receptor kinase defect can lead to this abnormality of insulin action kinetics, it also remains possible that this is attributable to a postreceptor abnormality in insulin action.

Taken together, these results indicate that the hyperinsulinemic dog is, indeed, a chronic model of peripheral insulin resistance. The model resembles certain features of the pre-NIDDM patient, since hyperinsulinemia and insulin resistance frequently precede the development of NIDDM, long before the deterioration of glucose tolerance (5, 6). Furthermore, decreased IR-TKA exists in the PVD dogs and is also a feature of NIDDM in humans (7). Therefore, further study of this dog model could prove useful for further understanding the pathophysiology of NIDDM or other insulin-resistant states.

In previous work, we have shown that in addition to steady state defects in insulin action, abnormalities of the kinetics of insulin action are important features of human insulin-resistant states (7, 8, 23). Our current studies show that kinetic abnormalities of insulin action are also a feature of hyperinsulinemia-induced insulin resistance. During the glucose clamp studies in normal dogs, the rate of rise of the arterial insulin concentration is very rapid, with a $t_{1/2}$a value of 2 min. The rate of rise of the interstitial insulin concentration (lymph insulin) is slower, due to the delay in transendothelial passage of insulin from the circulation to the interstitial space. In previous studies (12), we have shown in normal dogs that the rate of rise of lymph insulin is superimposable on the rate of activation of skeletal muscle insulin receptors and stimulation of glucose disposal, indicating that the appearance of insulin in the lymph accurately reflects the arrival of insulin at skeletal muscle sites of action, and that binding to and activation of the insulin receptor, as well as stimulation of the processes necessary for normal glucose disposal, are very rapid. To support these conclusions, it is necessary to assess accurately the appearance of interstitial insulin at the muscle. This was achieved by measuring lymph insulin sampled via the thoracic duct, a validated technique based on a simple rationale. Receptor-bound insulin is in equilibrium with that of interstitial fluid, and lymph is derived from interstitial fluid; therefore, changes in lymph insulin concentration are an estimate of moment-to-moment changes in insulin receptor binding (24). This is not to say that lymph insulin comes only from interstitial fluid bathing muscle cells. Thoracic duct lymph is also derived from the splanchnic area (25). However, the good correlation between thoracic duct lymph insulin, hind limb lymph insulin, muscle IR-TKA, and total body GDR (12, 26) in normal, insulin-sensitive dogs suggests the methodology is appropriate.

In the insulin-resistant PVD animals, two striking changes in the kinetics of insulin action were observed. First, a larger discrepancy was seen between the rates of rise in arterial and lymph insulin in the PVD animals compared with controls, indicating that a defect in transendothelial passage of insulin had developed as a result of the hyperinsulinemic insulin-resistant state. The reason for the hindered movement of insulin across the endothelium is unknown, but clearly, this could be due to endothelial cell dysfunction induced by the hyperinsulinemic insulin-resistant state. Indeed, Baron and colleagues (27, 28) have presented data showing functional abnormalities of endothelial cells in human insulin-resistant states. Insulin receptors have been isolated from the endothelium, which suggests transendothelial insulin transport is receptor mediated (29, 30). Conversely, more recent work has shown that this process is not saturable (31), which argues against receptor-mediated transport and predicts the movement of insulin across the endothelium is simply concentration gradient–dependent diffusion. Another way in which endothelial dysfunction could cause delayed lymph insulin appearance has to do with muscle blood flow. Some reports have shown that elevated circulating insulin levels increase skeletal muscle blood flow (27, 32), and in insulin-resistant states such as NIDDM (28) and obesity (27), the vasodilatory response to insulin is reduced. This response is a direct effect of insulin on the vessel wall, and is independent of neural or metabolic influences (for a review, see reference 33). Thus, the impaired ability of insulin to stimulate blood flow in insulin-resistant humans is thought to represent endothelial cell dysfunction.

The second kinetic defect observed in the PVD animals was that the rate of activation of glucose disposal was substantially slower ($t_{1/2}$a, 66±10 min) than the rate of rise of lymph insulin ($t_{1/2}$a, 40±4 min). This indicates that once insulin arrives at its skeletal muscle sites of action in the insulin-resistant animals, there is a slower rate at which insulin stimulates the cellular processes necessary to achieve an increase in glucose disposal. Whether this is due to the defect in IR-TKA or some postreceptor abnormality of insulin action remains to be defined. Interestingly, we have observed previously a defect in the rate at which insulin activates glucose disposal in insulin-resistant obese (8, 23) and NIDDM (7) subjects, further suggesting that this canine model of insulin resistance may be relevant to alterations in insulin action seen in human insulin-resistant states.

Taking all the data together, both prereceptor and target cell mechanisms are responsible for the substantially longer time required to stimulate GDR in the insulin-resistant animals. Using the $t_{1/2}$a data to estimate the respective contributions of prereceptor versus cellular mechanisms, one can estimate that the delay in transendothelial insulin transport was responsible for one third of the defect in activation of GDR, while abnormalities in cellular kinetics of insulin action were responsible for the remaining two thirds.

An interesting finding in this study was the lack of hepatic insulin resistance. Despite the development of peripheral insulin resistance in the PVD group, the magnitude and rate of suppression of HGP by insulin remained normal. Typically, sensitivity of the periphery to insulin is matched by that of the liver, regardless of the presence of insulin resistance (7, 21, 34). It has been generally believed that portal levels of insulin and glucagon regulate the liver directly, but a convincing body of work has now established the importance of peripheral levels of insulin in the regulation of HGP (35–40). Prager et al. (34) and Bradley et al. (41) have proposed that insulin inhibits HGP primarily through an extrahepatic mechanism, whereby the major rate-limiting step is transendothelial insulin transport, the same event that limits the kinetics of insulin-stimulated GDR in skeletal muscle. In this event, insulin's effects on peripheral tissues would activate some feedback mechanism, possibly by inhibition of lipolysis, or gluconeogenic precursor release (39, 42), or generation of a neural or humoral signal (41), which in turn reduces HGP. Therefore, the similar temporal relationship between the kinetics of GDR and HGP in normal animals (21, 41) or humans (11) may reflect insulin acting through a peripheral mechanism to influence simultaneously both muscle and liver glucose metabolism. Nonetheless, we observed a dissociation between the action of insulin in the periphery and in the liver. One explanation may lie with our animal preparation, in which the portal/peripheral insulin gradient was reversed. Although insulin resistance was induced by creating chronic hyperinsulinemia in the systemic circulation, the blood of the portal vein supplying the liver was actually hypoinsulinemic. Therefore, it is likely that the liver remained sensitive to insulin because of the lack of hyperinsulinemic exposure. However, this explanation does not reconcile the observations of normal hepatic sensitivity with the concept of indirect regulation of hepatic glucose production. Despite the establishment of an indirect effect, a direct insulin effect on the liver may also exist. The work of Sindelar et al. (43) has indicated recently that both peripheral and portal mechanisms regulate hepatic glucose metabolism, and they can act independently of one another. In these studies, it would appear that the direct effects of insulin on the liver remain normal, leading to normal suppression of HGP.

The β cell response to experimental hyperinsulinemia is also of interest. Clearly, in this model, the systemic hyperinsulinemia results from decreased hepatic clearance of insulin due to the portal bypass, rather than enhanced insulin secretion. This is demonstrated by the fact that C-peptide levels were not increased in the PVD animals, despite the fact that insulin levels were elevated consistently throughout all testing procedures. For example, during the IVGTT, glucose levels were comparable between the control and PVD animals. The PVD animals were hyperinsulinemic at all time points, but insulin secretion, as measured by C-peptide levels, was, if anything, slightly decreased in the PVD group. Assuming that the β cell regulates insulin secretion primarily to achieve normal circulating glucose levels, these results indicate that the systemic hyperinsulinemia compensated for the peripheral insulin resistance to maintain normal glucose levels at normal rates of insulin secretion. Alternatively, one might interpret the temporal sequence to mean that the peripheral insulin resistance compensates for the hyperinsulinemia to prevent hypoglycemia. In any event, the IVGTT data show that for any given glucose input, β cell insulin secretion is relatively normal in the PVD animals, meaning that in this model the peripheral insulin resistance does not enhance intrinsic β cell function and may even result in a slight impairment.

In spite of the peripheral insulin resistance and impaired transendothelial insulin transport, the PVD animals remain glucose tolerant, as assessed by the normal rate of fall of plasma glucose during the IVGTT. The fact that the rate of decline in glucose was normal in the PVD animals can be explained by three factors. First, the early decline in glucose lev-

els during an IVGTT is due largely to the mass action effect of glucose on glucose uptake, which would be the same in both control and PVD animals. Second, the PVD animals were hyperinsulinemic, which would tend to compensate for the insulin resistance. Finally, in PVD animals, the insulin resistance was confined to peripheral stimulation of glucose uptake as well as transendothelial insulin passage, while insulin's ability to suppress hepatic glucose production was normal. Since the liver's ability to respond to insulin is normal, and since insulin does not have to transverse an endothelial barrier to arrive at its hepatic site of action, a normal effect of insulin on the liver would be expected during the IVGTT, contributing to the normal glucose levels during the test.

In summary, we have characterized the insulin resistance produced by chronic hyperinsulinemia in the dog. The prolonged elevation of basal insulin levels led to peripheral insulin resistance, as shown by a marked reduction in insulin-stimulated GDR, which was, at least in part, the result of decreased insulin receptor function. However, the animals remained glucose tolerant with normal β cell function, and insulin sensitivity of the liver was unaffected. The time required for GDR to reach a maximum insulin-stimulated response in the hyperinsulinemic animals increased twofold over the control animals. Both prereceptor and cellular events contributed to the reduced rate of activation of GDR. A defect in the movement of insulin across the endothelium and into the interstitial fluid was observed in the PVD animals, and this was responsible for about one third of the reduction in the rate of activation of GDR, while cellular defects in insulin action caused the remaining two thirds.

Acknowledgments

The authors would like to thank A. Bloom for her excellent surgical assistance and K. Polonsky of the Diabetes Research and Training Center, University of Chicago, for C-peptide analysis (supported by grant DK-20595 from the National Institutes of Health).

This work was supported in part by grants from the National Institutes of Health (DK-33649, DK-33651, DK-07494), and by the Veterans Administration Research Service, Department of Veterans Affairs, and the Whittier Diabetes Institute.

References

1. Groth, C.G. 1988. Pancreatic Transplantation. W.B. Saunders Co., Philadelphia.

2. Rizza, R.A., L.J. Mandarino, J. Genest, B.A. Baker, and J.E. Gerich. 1985. Production of insulin resistance by hyperinsulinaemia in man. *Diabetologia.* 28:70–75.

3. Martin, C., K.S. Desai, and G. Steiner. 1983. Receptor and postreceptor insulin resistance induced by in vivo hyperinsulinemia. *Can. J. Physiol. Pharmacol.* 61:802–807.

4. Radziuk, J., P. Barron, H. Najm, and J. Davis. 1993. The effect of systemic venous drainage of the pancreas on insulin sensitivity. *J. Clin. Invest.* 92: 1713–1721.

5. Harris, M.I. 1995. Epidemiologic studies on the pathogenesis of non-insulin-dependent diabetes mellitus (NIDDM). *Clin. Invest. Med.* 18:231–239.

6. Zimmet, P.Z. 1993. Hyperinsulinemia—how innocent a bystander? *Diabetes Care.* 16:56–70.

7. Nolan, J.J., B. Ludvik, J. Baloga, D. Reichart, and J.M. Olefsky. 1997. Mechanisms of the kinetic defect in insulin action in obesity and NIDDM. *Diabetes.* 46:994–1000.

8. Prager, R., P. Wallace, and J.M. Olefsky. 1986. In vivo kinetics of insulin action on peripheral glucose disposal and hepatic glucose output in normal and obese subjects. *J. Clin. Invest.* 78:472–481.

9. Yang, J.Y., I.D. Hope, M. Ader, and R.N. Bergman. 1989. Insulin transport across capillaries is rate limiting for insulin action in dogs. *J. Clin. Invest.* 84:1620–1628.

10. Freidenberg, G.R., S.L. Suter, R.R. Henry, D. Reichart, and J.M. Olefsky. 1991. In vivo stimulation of insulin receptor kinase in human skeletal muscle. Correlation with insulin-stimulated glucose disposal during euglycemic clamp studies. *J. Clin. Invest.* 87:2222–2229.

11. Freidenberg, G.R., S. Suter, R.R. Henry, J. Nolan, D. Reichart, and J.M. Olefsky. 1994. Delayed onset of insulin activation of human receptor kinase in vivo in human skeletal muscle. *Diabetes.* 43:118–126.

12. Miles, P.D.G., M. Levisetti, D. Reichart, M. Khoursheed, A.R. Moossa, and J.M. Olefsky. 1994. Kinetics of insulin action in vivo. Identification of rate-limiting steps. *Diabetes.* 44:947–953.

13. Miller, A.R., D. Barr, C.L. Marsh, E.J. Kryshak, P.C. Butler, R.A. Rizza, and J.D. Perkins. 1989. Diversion of the gastroduodenal vein: an in situ model of systemic insulin drainage. *Diabetes Res. Clin. Pract.* 7:109–114.

14. Finegood, D.T., R.N. Bergman, and M. Vranic. 1988. Modelling error and apparent isotope discrimination confound estimation of endogenous glucose production during euglycemic glucose clamps. *Diabetes.* 37:1025–1034.

15. Desbuquois, B., and G.D. Aurbach. 1971. Use of polyethylene glycol to separate free and antibody-bound peptide hormone in radioimmunoassays. *J. Clin. Endocrinol. Metab.* 33:732–738.

16. Revers, R.R., R. Fink, J. Griffin, J.M. Olefsky, and O.G. Kolterman. 1984. Influence of hyperglycemia on insulin's in vivo effects in type II diabetes. *J. Clin. Invest.* 73:664–672.

17. Polonsky, K., J. Jaspan, W. Pugh, D. Cohen, M. Schneider, T. Schwartz, A.R. Moossa, H. Tager, and A.H. Rubenstein. 1983. Metabolism of C-peptide in the dog. In vivo demonstration of the absence of hepatic extraction. *J. Clin. Invest.* 72:1114–1123.

18. Hagopian, W., E.G. Lever, D. Cohen, D. Emmanouel, A.R. Moossa, K. Polonsky, and J. Jaspan. 1983. Predominance of renal and absence of hepatic metabolism of pancreatic polypeptide in the dog. *Am. J. Physiol.* 245:E171–E177.

19. Bradley, D.C., G.M. Steil, and R.N. Bergman. 1993. Quantitation of measurement error with Optimal Segments: basis for adaptive time course smoothing. *Am. J. Physiol.* 264:E902–E911.

20. Steele, R. 1959. Influence of glucose loading and of injected insulin on hepatic glucose output. *Ann. NY Acad. Sci.* 82:420–430.

21. Finegood, D.T., R.N. Bergman, and M. Vranic. 1987. Estimation of endogenous glucose production during hyperinsulinemic euglycemic glucose clamps: comparison of unlabeled and labeled exogenous glucose infusates. *Diabetes.* 36:914–924.

22. Marshall, S., and J.M. Olefsky. 1980. Effects of insulin incubation on insulin binding, glucose transport, and insulin degradation by isolated rat adipocytes. Evidence for hormone-induced desensitization at the receptor and post-receptor level. *J. Clin. Invest.* 66:763–772.

23. Castillo, C., C. Bogardus, R. Bergman, P. Thuillez, and S. Lillioja. 1994. Interstitial insulin concentrations determine glucose uptake rates but not insulin resistance in lean and obese men. *J. Clin. Invest.* 93:10–16.

24. Renkin, E.M. 1979. Lymph as a measure of the composition of interstitial fluid. *In* Pulmonary Edema. A.P. Fishman and E.M. Renkin, editors. American Physiological Society, Bethesda. 145–159.

25. Steil, G.M., M.A. Meador, and R.N. Bergman. 1993. Thoracic duct lymph. Relative contribution from splanchnic and muscle tissue. *Diabetes.* 42: 720–731.

26. Poulin, R.A., G.M. Steil, D.M. Moore, M. Ader, and R.N. Bergman. 1994. Dynamics of glucose production and uptake are more closely related to insulin in hindlimb lymph than in thoracic duct lymph. *Diabetes.* 43:180–190.

27. Laakso, M., S.V. Edelman, G. Brechtel, and A.D. Baron. 1990. Decreased effect of insulin to stimulate skeletal muscle blood flow in obese man. A novel mechanism for insulin resistance. *J. Clin. Invest.* 85:1844–1852.

28. Laakso, M., S.V. Edelman, G. Brechtel, and A.D. Baron. 1992. Impaired insulin-mediated skeletal muscle blood flow in patients with NIDDM. *Diabetes.* 41:1076–1083.

29. King, G.L., and S.M. Johnson. 1985. Receptor-mediated transport of insulin across endothelial cells. *Science.* 227:1583–1586.

30. Bar, R.S., J.C. Hoak, and M.L. Peacock. 1978. Insulin receptors in human endothelial cells: indentification and characterization. *J. Clin. Endocrinol. Metabol.* 47:699–702.

31. Steil, G.M., M. Ader, D.M. Moore, K. Rebrin, and R.N. Bergman. 1996. Transendothelial insulin transport is not saturable in vivo. No evidence for a receptor-mediated process. *J. Clin. Invest.* 97:1497–1503.

32. Baron, A.D., and G. Brechtel. 1993. Insulin differentially regulates systemic and skeletal muscle vascular resistance. *Am. J. Physiol.* 265:E61–E67.

33. Baron, A.D. 1996. Insulin and the vasculature—old actors, new roles. *J. Investig. Med.* 44:406–412.

34. Prager, R., P. Wallace, and J.M. Olefsky. 1987. Direct and indirect effects of insulin to inhibit hepatic glucose output in obese subjects. *Diabetes.* 36: 607–611.

35. Ishida, T., Z. Chap, J. Chou, R.M. Lewis, C.J. Hartley, M.L. Entman, and J.B. Field. 1984. Effects of portal and peripheral venous insulin infusion on glucose production and utilization in depancreatized, conscious dogs. *Diabetes.* 33:984–990.

36. Kryshak, E.J., P.C. Butler, C. Marsh, A. Miller, D. Barr, K. Polonsky, J.D. Perkins, and R.A. Rizza. 1990. Pattern of postprandial carbohydrate me-

tabolism and effects of portal and peripheral insulin delivery. *Diabetes.* 39:142–148.

37. Kruszynska, Y.T., P.D. Home, and K.G.M.M. Alberti. 1985. Comparison of portal and peripheral insulin delivery on carbohydrate metabolism in streptozotocin-diabetic rats. *Diabetologia.* 28:167–171.

38. Ader, M., and R.N. Bergman. 1990. Peripheral effects of insulin dominate suppression of fasting hepatic glucose production. *Am. J. Physiol.* 258: E1020–E1032.

39. Giacca, A., S.J. Fisher, Z.Q. Shi, R. Gupta, H.L.A. Lickley, and M. Vranic. 1992. Importance of peripheral insulin levels for insulin-induced suppression of glucose production in depancreatized dogs. *J. Clin. Invest.* 90:1769–1777.

40. Ader, M., and R.N. Bergman. 1994. Importance of transcapillary insulin transport to dynamics of insulin action after intravenous glucose. *Am. J. Physiol.* 266:E17–E25.

41. Bradley, D.C., R.A. Poulin, and R.N. Bergman. 1993. Dynamics of hepatic and peripheral insulin effects suggest common rate-limiting step in vivo. *Diabetes.* 42:296–306.

42. Sindelar, D.K., C.A. Chu, M. Rohlie, D.W. Neal, L.L. Swift, and A.D. Cherrington. 1997. The role of fatty acids in mediating the effects of peripheral insulin on hepatic glucose production in the conscious dog. *Diabetes.* 46:187–196.

43. Sindelar, D.K., J.H. Balcom, C.A. Chu, D.W. Neal, and A.D. Cherrington. 1996. A comparison of the effects of selective increases in peripheral or portal insulin of hepatic glucose production in the conscious dog. *Diabetes.* 45: 1594–1604.